

Manipulating the direction of Einstein-Podolsky-Rosen steering

Zhongzhong Qin^{1,2}, Xiaowei Deng^{1,2}, Caixing Tian^{1,2}, Meihong Wang^{1,2}, Xiaolong Su^{1,2,*}, Changde Xie^{1,2}, and Kunchi Peng^{1,2}
¹*State Key Laboratory of Quantum Optics and Quantum Optics Devices, Institute of Opto-Electronics, Shanxi University, Taiyuan 030006, People's Republic of China*
²*Collaborative Innovation Center of Extreme Optics, Shanxi University, Taiyuan, Shanxi 030006, People's Republic of China*

Einstein-Podolsky-Rosen (EPR) steering exhibits an inherent asymmetric feature that differs from both entanglement and Bell nonlocality, which leads to one-way EPR steering. Although this one-way EPR steering phenomenon has been experimentally observed, the schemes to manipulate the direction of EPR steering have not been investigated thoroughly. In this paper, we propose and experimentally demonstrate three schemes to manipulate the direction of EPR steering, either by varying the noise on one party of a two-mode squeezed state (TMSS) or transmitting the TMSS in a noisy channel. The dependence of the direction of EPR steering on the noise and transmission efficiency in the quantum channel is analyzed. The experimental results show that the direction of EPR steering of the TMSS can be changed in the presented schemes. Our work is helpful in understanding the fundamental asymmetry of quantum nonlocality and has potential applications in future asymmetric quantum information processing.

I. INTRODUCTION

Einstein-Podolsky-Rosen (EPR) steering is an intriguing phenomenon predicted by quantum mechanics, that allows one party, say Alice, to steer the state of a distant party, Bob, by exploiting their shared entanglement [1–4]. EPR steering stands between entanglement [5] and Bell nonlocality [6] in the hierarchy of quantum correlations. Violation of the Bell inequality implies EPR steering in both directions, and EPR steering of any direction implies that the state is entangled. The converse implications are not true; i.e., entangled states are not necessarily steering states and steering does not imply violation of the Bell inequality [7]. In the view of quantum information processing, EPR steering can be regarded as a verifiable entanglement distribution by an untrusted party, while entangled states need both parties to trust each other, and the Bell nonlocality is valid on the premise that they distrust each other [8]. EPR steering has recently attracted increasing interest in quantum optics and quantum information communities [7–9]. For example, it has been recently realized that EPR steering provides security in one-sided device-independent quantum key distribution (1SDI-QKD) [10] and plays an operative role in channel discrimination [11] and teleamplification [12]. Recently, 1SDI-QKD has been experimentally implemented [13, 14].

In EPR steering, Alice's ability to steer Bob's state may not be equal to Bob's ability to steer Alice's state. There are situations where Alice can steer Bob's state but Bob can not steer Alice's state, or vice versa, which are

referred to as one-way EPR steering [15]. The demonstration of fundamentally asymmetric nonlocality is of foundational significance for studying complex effects of quantum mechanics and has potential applications in asymmetric quantum information processing. The one-way EPR steering was first demonstrated with a two-mode squeezed state (TMSS) [15] and then extended to a multipartite system [16]. Both of the above two experimental demonstrations were performed on Gaussian states with Gaussian measurements. Other measurement methods used to show the property of one-way EPR steering have been theoretically constructed, including general projective measurements [17], arbitrary finite-setting positive-operator-valued-measures (POVMs) [9], infinite-setting POVMs [18], and an infinite number of arbitrary projective measurements [19]. Recently, genuine one-way EPR steering was experimentally demonstrated by two groups independently [20, 21].

Although this one-way EPR steering phenomenon has been investigated extensively [7, 9, 15–26], the scheme to manipulate actively the direction of EPR steering has not been investigated thoroughly. In this paper, we propose and experimentally demonstrate three schemes to effectively manipulate the direction of EPR steering. Two schemes are implemented by adding noise to one party of a TMSS, and the third scheme is implemented by transmitting the TMSS over a noisy channel. The dependence of the direction of the one-way EPR steering upon the physical parameters is given, which offers a direct reference for practical applications of EPR steering.

The paper is organized as follows. We present the manipulation schemes in Sec. II. The details of the experiment are presented in Sec. III. In Sec. IV, we present the results and some discussion. Finally, we conclude the paper in Sec. V.

*Electronic address: suxl@sxu.edu.cn

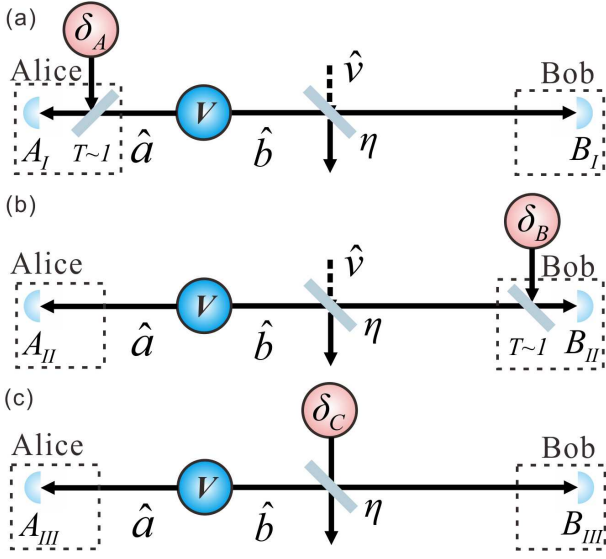


FIG. 1: Schematic of nontrivial manipulation schemes. (a) Manipulation scheme I. One mode of the TMSS is transmitted over a lossy channel to Bob's station and the loss is modeled by a beam splitter with transmission efficiency η . Vacuum state $\hat{\nu}$ is coupled into the signal channel through another input port of the beam splitter. In this case, Alice adds a Gaussian noise with variance δ_A to her state by using a beam splitter with transmission efficiency approaching unity. Alice and Bob make measurements on the amplitude and phase quadratures \hat{X}_A, \hat{P}_A and \hat{X}_B, \hat{P}_B of two remote modes by homodyne detectors, respectively. V represents the variance of one mode of the TMSS. (b) Manipulation scheme II. Bob adds a Gaussian noise with variance δ_B to his state by using a beam splitter with transmission efficiency approaching unity. (c) Manipulation scheme III. One mode of the TMSS is transmitted in a noisy channel with an excess noise higher than the vacuum noise. The excess noise with variance δ_C is coupled to the state through the beamsplitter.

II. MANIPULATION SCHEMES

The variance of each party in a symmetric TMSS is $V = \text{Cosh}2r$, where $r \in [0, \infty)$ is the squeezing parameter. All Gaussian properties of the TMSS state can be determined by the covariance matrix

$$\sigma_{AB} = \begin{pmatrix} \alpha & 0 & \gamma & 0 \\ 0 & \alpha & 0 & -\gamma \\ \gamma & 0 & \beta & 0 \\ 0 & -\gamma & 0 & \beta \end{pmatrix} = \begin{pmatrix} \alpha I & \gamma Z \\ \gamma Z & \beta I \end{pmatrix}, \quad (1)$$

with the matrix element $\sigma_{ij} = \langle \hat{\xi}_i \hat{\xi}_j + \hat{\xi}_j \hat{\xi}_i \rangle / 2 - \langle \hat{\xi}_i \rangle \langle \hat{\xi}_j \rangle$, where $\hat{\xi} \equiv (\hat{X}_A, \hat{P}_A, \hat{X}_B, \hat{P}_B)$ is the vector of the field quadratures, including the amplitude ($\hat{X} = \hat{a} + \hat{a}^\dagger$) and phase [$\hat{P} = (\hat{a} - \hat{a}^\dagger)/i$] quadratures of Alice's and Bob's modes. I and Z are the Pauli matrices:

$$I = \begin{pmatrix} 1 & 0 \\ 0 & 1 \end{pmatrix}, \quad Z = \begin{pmatrix} 1 & 0 \\ 0 & -1 \end{pmatrix}. \quad (2)$$

Note that the submatrices $\sigma_A = \alpha I$ and $\sigma_B = \beta I$ are the covariance matrices corresponding to the states of Alice's and Bob's subsystems, respectively. The TMSS is a symmetric state and an asymmetric state when $\sigma_A = \sigma_B$ and $\sigma_A \neq \sigma_B$, respectively.

EPR steering for bipartite Gaussian states of continuous variable systems can be quantified by [27]

$$\mathcal{G}^{A \rightarrow B}(\sigma_{AB}) = \max \left\{ 0, \frac{1}{2} \ln \frac{\det \sigma_A}{\det \sigma_{AB}} \right\}, \quad (3)$$

where σ_A and σ_{AB} are the covariance matrices corresponding to Alice's state and the TMSS state, respectively. $\mathcal{G}^{A \rightarrow B}(\sigma_{AB}) > 0$ represents that Alice has the ability to steer Bob's state. Similarly, we have

$$\mathcal{G}^{B \rightarrow A}(\sigma_{AB}) = \max \left\{ 0, \frac{1}{2} \ln \frac{\det \sigma_B}{\det \sigma_{AB}} \right\}, \quad (4)$$

which represents Bob's ability to steer Alice's state, where σ_B is the covariance matrix of Bob's state. From the expressions of $\mathcal{G}^{A \rightarrow B}(\sigma_{AB})$ and $\mathcal{G}^{B \rightarrow A}(\sigma_{AB})$, it can be seen that Alice and Bob have the same steerability if $\det \sigma_A = \det \sigma_B$ is satisfied; i.e., the bipartite Gaussian state is a symmetric state. If the state is an asymmetric state, the steerabilities of Alice and Bob will be different.

As shown in Fig. 1(a), in manipulation scheme I, Alice adds the Gaussian noise \hat{N}_A with variance δ_A to her state. In this case, the modes at Alice's and Bob's stations are $\hat{A}_I = \hat{a} + \hat{N}_A$ and $\hat{B}_I = \sqrt{\eta} \hat{b} + \sqrt{1-\eta} \hat{\nu}$, respectively. So we have $\alpha_I = V + \delta_A$, $\beta_I = \eta V + (1-\eta)$, and $\gamma_I = \sqrt{\eta(V^2 - 1)}$ in the covariance matrix, where the variances of the amplitude and phase quadratures for the thermal and vacuum states are $\Delta^2(\hat{X}_{N_A}) = \Delta^2(\hat{P}_{N_A}) = \delta_A$ and $\Delta^2(\hat{X}_\nu) = \Delta^2(\hat{P}_\nu) = 1$, respectively.

As shown in Fig. 1(b), in manipulation scheme II, Bob adds the Gaussian noise \hat{N}_B with variance δ_B to his state after the transmission of mode \hat{b} over a lossy channel. In this case, the modes at Alice's and Bob's stations are $\hat{A}_{II} = \hat{a}$ and $\hat{B}_{II} = \sqrt{\eta} \hat{b} + \sqrt{1-\eta} \hat{\nu} + \hat{N}_B$, respectively. So we have $\alpha_{II} = V$, $\beta_{II} = \eta V + (1-\eta) + \delta_B$, and $\gamma_{II} = \sqrt{\eta(V^2 - 1)}$ in the covariance matrix.

In EPR steering, Alice can steer Bob's state, which means that Alice can infer Bob's state, and vice versa. In the case with unit transmission efficiency, if noises are added to Alice's state, the uncertainty of Alice's state predicted by Bob will increase, and thus the difficulty for Bob to steer Alice's state will also increase and Bob will lose the ability to steer Alice's state when the added noise is high enough. However, in this case Alice still can steer Bob's state because the noise is added by herself and she can easily remove the influence of the noise as needed. The analysis is also appropriate to manipulation scheme II.

The one-way EPR steering has been demonstrated in a lossy channel previously [15, 16]. Besides the lossy channel, there is also another kind of quantum channel, i.e., the noisy channel. In a lossy but noiseless quantum channel, the noise induced by loss is nothing but the vacuum noise (corresponding to a zero-temperature environment). While in a noisy channel, excess noise higher

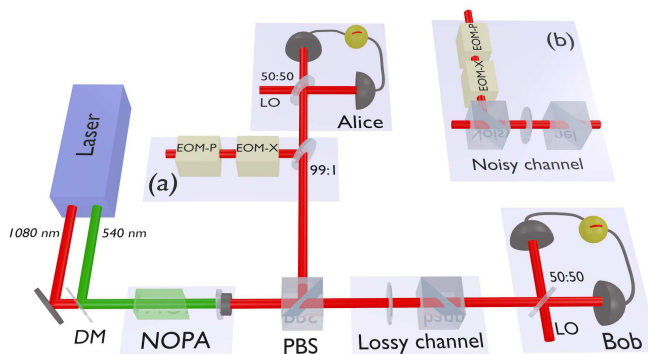


FIG. 2: Schematic of the experimental setup. Laser beams at 540 and 1080 nm from a dual-wavelength laser are used as the pump and seed beams of a NOPA, respectively. Homodyne detections are performed at Alice's and Bob's stations, respectively. A half-wave plate and PBS are used to adjust the transmission efficiency of the channel to Bob's station. Noise at Alice's (or Bob's) station is added by mixing the signal with an auxiliary beam on a high transmissivity beamsplitter (99:1), where the Gaussian white noises are modulated on the auxiliary beam by EOMs [Inset (a)]. The noisy channel is modeled by combining the signal channel and another auxiliary beam modulated by EOMs at a PBS followed by another half-wave plate and a PBS [Inset (b)]. DM, dichroic mirror; NOPA, nondegenerate optical parametric amplifier; LO, local oscillator; EOM, Electro-optic modulator.

than the vacuum noise exists [28]. It has been shown that the excess noise in the quantum channel will limit the transmission distance of quantum key distribution with continuous variables [28]. As shown in Fig. 1(c), in manipulation scheme III, we consider EPR steering of a TMSS in a noisy channel. After mode \hat{b} is transmitted through the noisy channel with excess noise \hat{N}_C , the modes at Alice's and Bob's stations are $\hat{A}_{III} = \hat{a}$ and $\hat{B}_{III} = \sqrt{\eta}\hat{b} + \sqrt{1-\eta}(\hat{N}_C + \hat{v})$, respectively. The variances of the amplitude and phase quadratures of excess noise are $\Delta^2(\hat{X}_{N_C}) = \Delta^2(\hat{P}_{N_C}) = \delta_C$. $\delta_C = 0$ means that there is no the excess noise, and only loss exists in the channel. $\delta_C > 0$ means that there excess noise exists in the channel. So we have $\alpha_{III} = V$, $\beta_{III} = \eta V + (1-\eta)(\delta_C + 1)$, and $\gamma_{III} = \sqrt{\eta(V^2 - 1)}$ in the covariance matrix.

III. DETAILS OF THE EXPERIMENT

Figure 2 shows the schematic of the experimental setup. The nondegenerate optical parametric amplifier (NOPA) consists of an α -cut type-II KTP crystal and a concave mirror. The front face of the KTP crystal is coated to be used as the input coupler, and the concave mirror serves as the output coupler [29]. The transmissivities of the input coupler at 540 and 1080 nm are 21.2% and 0.04%, respectively. The transmissivities of the output coupler at 540 nm and 1080 nm are 0.5% and 12.5%,

respectively. The end face of the KTP crystal is cut to 1° along the y - z plane of the crystal and is antireflection coated for both 1080 and 540 nm, so that triple resonance of the pump and the two subharmonic modes can be realized by tuning the temperature and the position of the KTP crystal [30]. A nearly pure -3 dB TMSS is generated by NOPA.

In manipulation scheme I, Alice adds Gaussian noise to her state. The other mode of the TMSS is transmitted to Bob through a lossy channel. In the demonstration of manipulation scheme II, the noise addition part [Fig. 2, inset (a)] is moved to Bob's state. In the demonstration of the manipulation scheme III, the lossy channel is replaced by a noisy channel [Fig. 2, inset (b)].

IV. RESULTS AND DISCUSSIONS

Figures 3(a), 3(b), and 3(c) show the EPR steering regions for $\mathcal{G}^{A \rightarrow B}(\sigma_{AB}) \geq 0$ and $\mathcal{G}^{B \rightarrow A}(\sigma_{AB}) \geq 0$ parametrized by the transmission efficiency η and the noise (δ_A , δ_B , and δ_C) corresponding to manipulation schemes I, II, and III, respectively. As shown in Fig. 3(a), two-way EPR steering (region I) can be turned to full one-way EPR steering $A \rightarrow B$ (region II) as the noise added to Alice's state δ_A exceeds the boundary $\delta_A = \frac{(V-1)(2\eta-1)}{1-\eta+V\eta}$ (blue curve). In region II, Alice can steer Bob's state while Bob cannot steer Alice's state. This shows that Alice stops Bob from steering her state by adding noise to her state (while she still can steer Bob's state). The maximum noise added to Alice's state for one-way EPR steering $A \rightarrow B$ is $\delta_A = 1$.

As shown in Fig. 3(b), if Bob adds noise to his state, the two-way EPR steering can be turned to either one-way EPR steering $A \rightarrow B$ (region II) or $B \rightarrow A$ (region III), depending on the transmission efficiency η and the noise level δ_B added by himself. The boundary between two-way and one-way EPR steering $A \rightarrow B$ ($B \rightarrow A$) is given by $\delta_B = 2\eta - 1$ [$\delta_B = \frac{(V-1)\eta}{V}$]. The crossover point at $(\eta = \frac{V}{1+V}, \delta_B = \frac{V-1}{V+1})$ corresponds to the boundary of changing the direction of one-way EPR steering. This shows that Bob can stop Alice from steering his state by adding noise to his state in some region.

When one mode of a TMSS is transmitted in a noisy channel, Alice's one-way EPR steering can survive iff $\delta_C < V - 1$ and $\eta < \frac{V}{1+V}$ [region II in Fig. 3(c)], and Bob can achieve the one-way EPR steering in a channel with the excess noise $\frac{\eta(V-1)}{V(1-\eta)} < \delta_C < \frac{2\eta-1}{1-\eta}$ as long as $\eta > \frac{V}{1+V}$ [region III in Fig. 3(c)]. The boundary between two-way and one-way EPR steering for $A \rightarrow B$ ($B \rightarrow A$) is given by $\delta_C = \frac{2\eta-1}{1-\eta}$ [$\delta_C = \frac{\eta(V-1)}{V(1-\eta)}$]. The crossover point at $(\eta = \frac{V}{1+V}, \delta_C = V - 1)$ corresponds to the boundary of changing the direction of one-way EPR steering. This shows that the direction of EPR steering is influenced by the amount of excess noise in the quantum channel.

In order to quantify the steerabilities of Alice and Bob, the dependence of EPR steering on transmission

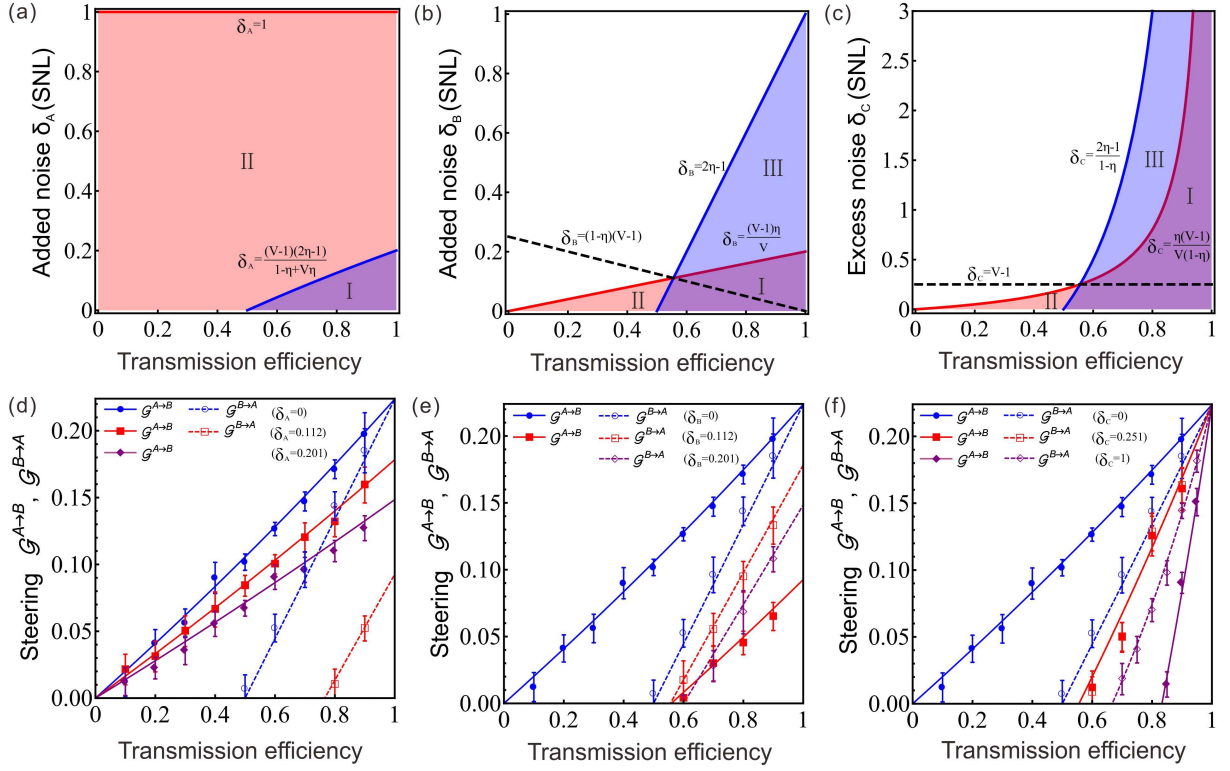


FIG. 3: Calculated parameter dependencies of EPR steering direction and experimental results. (a)-(c) Different regions of EPR steering for a TMSS with noise added to Alice's state, Bob's state, and the channel to Bob's station, respectively. The unit of noise is the shot noise level (SNL). Red curves and blue curves represent boundaries for $\mathcal{G}^{A \rightarrow B}(\sigma_{AB}) \geq 0$ and $\mathcal{G}^{B \rightarrow A}(\sigma_{AB}) \geq 0$ in three different cases, respectively. Region I corresponds to two-way steering $A \leftrightarrow B$, while regions II and III correspond to one-way EPR steering $A \rightarrow B$ and $B \rightarrow A$, respectively. The black dashed line $\delta_B = (1-\eta)(V-1)$ in panel (b) and $\delta_C = V-1$ in panel (c) represent the condition for $\det \sigma_A = \det \sigma_B$, i.e., $\mathcal{G}^{A \rightarrow B} = \mathcal{G}^{B \rightarrow A}$. (d)-(f) Quantum steering of a TMSS as a function of transmission efficiency η , with different amounts of noise added to Alice's state, Bob's state, and the channel to Bob's station, respectively. Solid lines and dashed lines show theoretical predictions of $\mathcal{G}^{A \rightarrow B}$ and $\mathcal{G}^{B \rightarrow A}$, respectively. Blue lines in the three cases represent the situation in which there is no noise added ($\delta_{A,B,C} = 0$) but only the loss exists. Red lines and purple lines in panel (d) [panel (e)] represent $\delta_A = 0.112$ [$\delta_B = 0.112$] and $\delta_A = 0.201$ [$\delta_B = 0.201$], respectively. Red lines and purple lines in (f) represent $\delta_C = 0.251$ and $\delta_C = 1$, respectively. The variance of the original TMSS is chosen to be $V = 1.251$ in theoretical predictions, corresponding to -3 dB squeezing. Error bars of experimental data represent 1 standard deviation and are obtained based on the statistics of the measured data.

efficiency at different noise levels and the corresponding experimental data are shown in Figs. 3(d), 3(e), and 3(f), respectively. The steerabilities of Alice and Bob at different transmission efficiencies are calculated from the experimentally measured covariance matrices, which are obtained by homodyne measurements on Alice's and Bob's modes [31].

The maximum EPR steering is obtained when there is no loss ($\eta = 1$) and noise ($\delta_{A,B,C} = 0$), and the steerabilities of Alice and Bob are the same since the TMSS is a symmetric state in this case. In manipulation scheme I [Fig. 3(d)], as δ_A increases to 0.112, both $\mathcal{G}^{A \rightarrow B}$ and $\mathcal{G}^{B \rightarrow A}$ decrease. However, Alice's one-way EPR steering range increases from $0 < \eta < 0.5$ to $0 < \eta < 0.768$. As δ_A increases to 0.201, Alice obtains one-way steerability in the whole transmission efficiency range. This result confirms that Alice stops Bob from steering her state under certain conditions by making local actions (adding noise

to her state).

In manipulation scheme II [Fig. 3(e)], as δ_B increases to 0.112, $\mathcal{G}^{B \rightarrow A}$ is always larger than $\mathcal{G}^{A \rightarrow B}$ at different transmission efficiencies, and they decrease to zero at the same transmission efficiency $\eta = 0.556$, which means that Alice's and Bob's EPR steering ranges are the same. As δ_B increases to 0.201, Bob obtains one-way steerability in the range of $0.601 < \eta < 1$. This result confirms that Bob stops Alice from steering his state under certain conditions by making local actions (adding noise to his state).

In manipulation scheme III [Fig. 3(f)], $\mathcal{G}^{A \rightarrow B}$ and $\mathcal{G}^{B \rightarrow A}$ overlap with $\delta_C = 0.251$, which corresponds to the case where $\delta_C = V-1$ is satisfied [the black dashed line shown in Fig.3 (c)], and they decrease to zero at the same transmission efficiency of $\eta = 0.558$. As δ_C increases to 1, Bob's steerability is always larger than that of Alice, and Bob obtains one-way steering in the trans-

mission efficiency range of $0.667 < \eta < 0.823$. This result confirms that the direction of EPR steering is changed in a noisy channel.

Here, we discuss the physical reason for the change of the EPR steering direction in a Gaussian TMSS. One-way EPR steering is related to the asymmetric property of the TMSS. From the expression of $\mathcal{G}^{A \rightarrow B}(\sigma_{AB})$ and $\mathcal{G}^{B \rightarrow A}(\sigma_{AB})$, it can be clearly seen that the conditions corresponding to EPR steering regions I, II, and III are $\det \sigma_A \& \det \sigma_B > \det \sigma_{AB}$, $\det \sigma_A > \det \sigma_{AB} > \det \sigma_B$, and $\det \sigma_B > \det \sigma_{AB} > \det \sigma_A$, respectively. Two-way EPR steering can be transformed to one-way EPR steering $A \rightarrow B$ ($B \rightarrow A$) if the asymmetry of the state exceeds the boundary $\det \sigma_{AB} = \det \sigma_B$ ($\det \sigma_{AB} = \det \sigma_A$) between regions I and II (regions I and III). However, it must be pointed out that the asymmetric property of the TMSS is only a necessary condition for one-way EPR steering. In other words, a TMSS exhibiting one-way EPR steering must be an asymmetric state, while a TMSS exhibiting two-way EPR steering may also be an asymmetric state.

The presented manipulation schemes can be connected with one of the applications of EPR steering, the 1SDI-QKD scheme. The security of 1SDI-QKD depends on the direction of EPR steering. For example, ‘‘Alice must demonstrate steering of Bob’s state’’ if Alice’s measurement device is untrusted while Bob’s is trusted [10]. In manipulation scheme I, Alice’s manipulation can be regarded as part of a legitimate step of a QKD protocol. In this case, Alice gets full one-way EPR steering over the whole transmission efficiency range ($0 < \eta < 1$) by adding noise to her state. Manipulation schemes II and III can be regarded as attacks from an adversarial party. In manipulation scheme II, Bob obtains one-way steering ability under certain conditions by making local actions (it can also be done by an adversarial party in the attack). The change of EPR steering direction may lead to

the change of role of the communication parties in 1SDI-QKD, which may influence the security of 1SDI-QKD. It has been shown that the secure transmission distance of 1SDI-QKD is limited by excess noise in the quantum channel [14]. In manipulation scheme III, by investigating the direction of EPR steering in a noisy channel, we show that the excess noise results in the change of the direction of EPR steering, which provides the physical reason for limiting the secure transmission distance of 1SDI-QKD caused by excess noise.

V. CONCLUSION

In summary, three schemes to actively manipulate the direction of EPR steering are demonstrated. The manipulation schemes are implemented either by varying the noise on one party of a TMSS or by transmitting the TMSS in a noisy channel. We show that the direction of EPR steering is related to the asymmetry of a TMSS. The change of EPR steering direction depends on the noise level and the transmission efficiency of the quantum channel in different manipulation schemes. The experimental results confirm that the direction of EPR steering of the TMSS can be changed in the presented schemes. Our work is helpful in understanding the fundamental asymmetry of EPR steering and has potential applications in asymmetric quantum information processing.

This research was supported by the NSFC (Grant Nos. 11522433, 61601270, and 61475092), the program of Youth Sanjin Scholar, the applied basic research program of Shanxi province (Grant No. 201601D202006) and National Basic Research Program of China (Grant No. 2016YFA0301402).

Z. Qin and X. Deng contributed equally to this work.

-
- [1] A. Einstein, B. Podolsky, and N. Rosen, Can quantum-mechanical description of physical reality be considered complete? *Phys. Rev.* **47**, 777 (1935).
 - [2] E. Schrödinger, Discussion of probability relations between separated systems, *Proc. Cambridge Philos. Soc.* **31**, 555 (1935).
 - [3] E. Schrödinger, Probability relations between separated systems, *Proc. Cambridge Philos. Soc.* **32**, 446 (1936).
 - [4] D. J. Saunders, S. J. Jones, H. M. Wiseman, and G. J. Pryde, Experimental EPR-steering using Bell-local states. *Nat. Phys.* **6**, 845 (2010).
 - [5] R. Horodecki, P. Horodecki, M. Horodecki, and K. Horodecki, Quantum entanglement, *Rev. Mod. Phys.* **81**, 865 (2009).
 - [6] J. S. Bell, On the Einstein Podolsky Rosen paradox, *Physics* **1**, 195 (1964).
 - [7] H. M. Wiseman, S. J. Jones, and A. C. Doherty, Steering, entanglement, nonlocality, and the Einstein-Podolsky-Rosen paradox, *Phys. Rev. Lett.* **98**, 140402 (2007).
 - [8] S. J. Jones, H. M. Wiseman, and A. C. Doherty, Entanglement, Einstein-Podolsky-Rosen correlations, Bell nonlocality, and steering, *Phys. Rev. A* **76**, 052116 (2007).
 - [9] P. Skrzypczyk, M. Navascués, and D. Cavalcanti, Quantifying Einstein-Podolsky-Rosen steering, *Phys. Rev. Lett.* **112**, 180404 (2014).
 - [10] C. Branciard, E. G. Cavalcanti, S. P. Walborn, V. Scarani, and H. M. Wiseman, One-sided device-independent quantum key distribution: Security, feasibility, and the connection with steering, *Phys. Rev. A* **85**, 010301 (2012).
 - [11] M. Piani and J. Watrous, Necessary and sufficient quantum information characterization of Einstein-Podolsky-Rosen steering, *Phys. Rev. Lett.* **114**, 060404 (2015).
 - [12] Q. He, L. Rosales-Zárate, G. Adesso, and M. D. Reid, Secure continuous variable teleportation and Einstein-Podolsky-Rosen steering, *Phys. Rev. Lett.* **115**, 180502 (2015).
 - [13] T. Gehring *et al.*, Implementation of continuous-variable

- quantum key distribution with composable and one-sided-device-independent security against coherent attacks. *Nat. Commun.* **6**, 8795 (2015).
- [14] N. Walk *et al.*, Experimental demonstration of Gaussian protocols for one-sided device-independent quantum key distribution. *Optica* **3**, 634 (2015).
- [15] V. Händchen, T. Eberle, S. Steinlechner, A. Sambrowski, T. Franz, R. F. Werner, and R. Schnabel, Observation of one-way Einstein-Podolsky-Rosen steering, *Nat. Photonics* **6**, 596 (2012).
- [16] S. Armstrong, M. Wang, R. Y. Teh, Q. H. Gong, Q. Y. He, J. Janousek, H.-A. Bachor, M. D. Reid, and P. K. Lam, Multipartite Einstein-Podolsky-Rosen steering and genuine tripartite entanglement with optical networks, *Nat. Phys.* **11**, 167 (2015).
- [17] J. Bowles, T. Vértesi, M. T. Quintino, and N. Brunner, One-way Einstein-Podolsky-Rosen steering. *Phys. Rev. Lett.* **112**, 200402 (2014).
- [18] M. T. Quintino, T. Vértesi, D. Cavalcanti, R. Augusiak, M. Demianowicz, A. Acín, and N. Brunner, Inequivalence of entanglement, steering, and Bell nonlocality for general measurements, *Phys. Rev. A* **92**, 032107 (2015).
- [19] D. A. Evans and H. M. Wiseman, Optimal measurements for tests of Einstein-Podolsky-Rosen steering with no detection loophole using two-qubit Werner states, *Phys. Rev. A* **90**, 012114 (2014).
- [20] S. Wollmann, N. Walk, A. J. Bennet, H. M. Wiseman, and G. J. Pryde, Observation of genuine one-Way Einstein-Podolsky-Rosen steering, *Phys. Rev. Lett.* **116**, 160403 (2016).
- [21] K. Sun, X. Ye, J. Xu, X. Xu, J. Tang, Y. Wu, J. Chen, C. Li, and G. Guo, Experimental quantification of asymmetric Einstein-Podolsky-Rosen steering, *Phys. Rev. Lett.* **116**, 160404 (2016).
- [22] S. L. W. Midgley, A. J. Ferris, and M. K. Olsen, Asymmetric Gaussian steering: when Alice and Bob disagree, *Phys. Rev. A* **81**, 022101 (2010).
- [23] C. Lee, S. Ji, and H. Nha, Quantum steering for continuous-variable states, *J. Opt. Soc. Am. B* **30**, 2483 (2013).
- [24] L. Rosales-Zárate, R. Y. Teh, S. Kieseewetter, A. Broils, K. Ng, and M. D. Reid, Decoherence of Einstein-Podolsky-Rosen steering, *J. Opt. Soc. Am. B* **32**, A82 (2015).
- [25] Q. Y. He, Q. H. Gong, and M. D. Reid, Classifying directional Gaussian entanglement, Einstein-Podolsky-Rosen steering, and discord, *Phys. Rev. Lett.* **114**, 060402 (2015).
- [26] T. Guerreiro *et al.*, Demonstration of Einstein-Podolsky-Rosen steering using single-photon path entanglement and displacement-based detection. *Phys. Rev. Lett.* **117**, 070404 (2016).
- [27] I. Kogias, A. R. Lee, S. Ragy, and G. Adesso, Quantification of Gaussian quantum steering, *Phys. Rev. Lett.* **114**, 060403 (2015).
- [28] C. Weedbrook *et al.*, Gaussian quantum information. *Rev. Mod. Phys.* **84**, 621-669 (2012).
- [29] X. Su *et al.*, Gate sequence for continuous variable one-way quantum computation. *Nat. Commun.* **4**, 2828 (2013).
- [30] Y. Zhou, X. Jia, F. Li, C. Xie, and K. Peng, Experimental generation of 8.4 dB entangled state with an optical cavity involving a wedged type-II nonlinear crystal, *Opt. Express* **23**, 4952 (2015).
- [31] S. Steinlechner, J. Bauchrowitz, T. Eberle, and R. Schnabel, Strong Einstein-Podolsky-Rosen steering with unconditional entangled states. *Phys. Rev. A* **87**, 022104 (2013).